



CHORUS

This is the accepted manuscript made available via CHORUS. The article has been published as:

Spatial Correlations and the Insulating Phase of the High- T_c Cuprates: Insights from a Configuration-Interaction-Based Solver for Dynamical Mean Field Theory

Ara Go and Andrew J. Millis

Phys. Rev. Lett. **114**, 016402 — Published 6 January 2015

DOI: [10.1103/PhysRevLett.114.016402](https://doi.org/10.1103/PhysRevLett.114.016402)

Spatial correlations and the insulating phase of the high- T_c cuprates: insights from a configuration interaction based solver for dynamical mean field theory

Ara Go and Andrew J. Millis

Department of Physics, Columbia University in the City of New York, New York, NY 10027

(Dated: December 2, 2014)

A recently proposed configuration-interaction based impurity solver is used in combination with the single-site and four-site cluster dynamical mean field approximations to investigate the three-band copper oxide model believed to describe the electronic structure of high transition temperature copper-oxide superconductors. Use of the configuration interaction solver enables verification of convergence of results with respect to number of bath orbitals. The spatial correlations included in the cluster approximation substantially shift the metal-insulator phase boundary relative to the prediction of the single-site approximation and increase the predicted energy gap of the insulating phase by about 1eV above the single-site result. Vertex corrections occurring in the four-site approximation act to dramatically increase the value of the optical conductivity near the gap edge, resulting in a much agreement with data. The calculations reveal two distinct correlated insulating states: the ‘magnetically correlated insulator’, in which nontrivial intersite correlations play an essential role in stabilizing the insulating state, and the strongly correlated insulator, in which local physics suffices. Comparison of the calculations to data place the cuprates in the magnetically correlated Mott insulator regime.

Understanding “strongly correlated” electron physics [1] is one of the grand challenges of condensed matter theory. The layered copper-oxide materials such as $\text{La}_{2-x}\text{Sr}_x\text{CuO}_4$ are central to this endeavor because they exhibit a range of unusual electronic properties including both high transition temperature superconductivity and a correlation-driven insulating phase. Indeed the physics that causes the insulating behavior is believed [2] also to give rise to other important correlated electron properties, in particular, superconductivity. A clear understanding of the physics of insulating phase is therefore essential. A basic question in the field is whether the local effects of strong correlations are sufficient to describe the important properties [2–5] or whether intersite correlations are essential to the description of the observed properties [6–9]. In this paper we use a cluster implementation [10] of dynamical mean field theory [11] to address the issue of the physics of the insulating phase of the cuprates. A crucial role in our work is played by the configuration interaction (CI) solver introduced by Zgid, Gull and Chan [12, 13], which enables the computation of converged real-frequency single particle and optical spectra for wide parameter ranges including both strong and weak interactions. We find that the “copper-oxygen model” which is generally believed [14–16] to represent the basic electronic physics of the cuprates has three distinct regimes of behavior: a metal, a charge transfer insulator and a magnetically correlated charge transfer insulator in which the insulating behavior is due to intersite correlators and not to the standard local Mott physics. Comparison of our results to data locates the cuprates in the magnetically mediated insulator regime.

An appropriate ‘microscopic’ Hamiltonian for the ma-

terials is $H_{CT} = H_d + H_{rest}$

$$H_d = \sum_{k\sigma} \varepsilon_d d_{k\sigma}^\dagger d_{k\sigma} + U \sum_i n_{d,i\uparrow} n_{d,i\downarrow} \quad (1)$$

$$H_{rest} = \sum_{ka\sigma} t_{pd}^a(k) d_{k\sigma}^\dagger p_{k,\sigma}^a + H.c. + \sum_{kab\sigma} \varepsilon_k^{ab} p_{k\sigma}^{a\dagger} p_{k\sigma}^b \quad (2)$$

where k is a momentum in the two dimensional Brillouin zone, $d_{k\sigma}^\dagger$ creates an electron of momentum k in a Cu orbital and $p_{k\sigma}^{a\dagger}$ creates an electron in one of the two in-plane oxygen p_σ -orbitals. The charge transfer parameter Δ is defined as the difference between the unrenormalized on-site copper energy ε_d and the average on-site oxygen energy $\varepsilon_p = \frac{1}{2} \text{Tr}_{kab} \varepsilon_k^{ab}$ as $\Delta = \varepsilon_p - \varepsilon_d$.

The parameters of H_{CT} may be derived e.g. from Wannier function fits to a band calculation; however the d energy ε_d must be renormalized by a “double counting correction” whose magnitude is not theoretically known [17]. Previous work [9] has shown that the behavior of the model does not depend on the details of the oxygen dispersion ε_k^{ab} or on how the double counting is implemented. The only important variable is the d -occupancy $N_d = \langle d_{i\sigma}^\dagger d_{i\sigma} \rangle$, which of course depends on these variables in a complicated way. In this paper we therefore adopt the most convenient model, $\varepsilon_k^{ab} = \varepsilon_p \delta_{ab}$, $t_{pd}^a(k) = 2i \sin k_a$ and regard the double counting correction (i.e. the p - d energy difference Δ) as a parameter of the theory.

We study H_{CT} using the single and four-site versions of the dynamical cluster approximation implementation of dynamical mean field theory [10] as applied to the three-band model e.g. by Macridin et al [18]. Previous work on the Hubbard model revealed large qualitative differences between the single-site and four-site cluster results [10, 19] with larger clusters providing important differences of detail but not changing the qualitative picture [19].

Less work has been done on cluster approximations to H_{CT} although the validity of the one-band model has been considered [18], and an interesting studies of the dependence of superconducting properties on the apical oxygen distance has appeared [5].

The central computational task in dynamical mean field theory [11] is the solution of a “quantum impurity model”, a 0-space plus 1-time dimensional quantum field theory or alternatively a small number N_c of interacting orbitals coupled to a non-interacting bath. The existing methods of solution are not fully satisfactory. Continuous-time quantum Monte-Carlo [20–22] has proven effective for the single-band Hubbard model at not too strong correlations [23] and for multiorbital situations in the single-site approximation [21, 24] but scales very poorly with system size in situations involving orbital degeneracy, becomes prohibitively expensive for strong correlations and suffers a severe sign problem in situations with more than one orbital and low point symmetry [22]. Also it is formulated in imaginary time and an ill-controlled analytical continuation process is required to obtain the real frequency information required for spectral functions. The numerical renormalization group [25] and the density matrix renormalization group [26] have been effective in special situations (for example determining the precise low frequency spectral properties of the single-orbital Hubbard model in the single-site approximation) but have proven difficult to apply generally. The exact diagonalization method of Caffarel and Krauth [27] and improved by Capone [28] approximates the quantum field theory as a finite-size Hamiltonian which is diagonalized using e.g. Lanczos methods, and although interesting studies have appeared [29–32] is limited by the number of sites available.

In this paper we use our implementation of a new method, the configuration interaction approach of Zgid and Chan [13], to study the metal-insulator phase diagram, electron spectral function and optical conductivity of a fundamental model of the high transition temperature CuO_2 -based superconducting materials. We use a zero temperature implementation. A related CI implementation has recently been used by Lin [33] to study defect and other properties of SrTiO_3 . The CI method is a variant of ED in which the full Hilbert space is not treated; rather, the diagonalization is performed in a variationally chosen subspace, allowing larger problems to be attacked. The details of our implementation will be given elsewhere [34]. Here we note that the ground state is found by minimizing the Hamiltonian in a subspace consisting of number N_{ref} of reference states plus all possible states containing up to P particle-hole pair excitations above the reference states. The key to the method is that P is small. We find that in general choosing up to two particle-hole pairs for each spin direction (this is a subset of all possible $P = 4$ states) suffices, and that for moderate interactions $U \lesssim 12\text{eV}$ simply restrict-

ing to $P = 2$ suffices.

The reference states are obtained in practice as follows. We define the natural orbital basis as the eigenstates of the single particle density matrix of the ground state $\hat{\rho} = |\psi\rangle\langle\psi|$. We choose as active orbitals the $2N_c$ single particle states of the natural orbital basis with ground-state occupancy closest to 1/2. The other orbitals are found to be a very good approximation to have occupancy 1 or 0. As also noted by Lin [33], this limited number of partially filled orbitals is crucial to the success of the method. The reference states are then defined as all many body states which may be formed from the $2N_c$ active orbitals with appropriate conserved quantities (these are particle number $N_{\text{act}} = N_c$ and, in the four-site calculations, spin $S_z = 0$) with the other orbitals remaining filled or empty. Since the reference states and the ground state depend on each other, the whole procedure is iterated until self-consistency is reached.

In this scheme the number N_{ref} of reference states is equal to the number of states in the largest $S_z = 0$ sector of the impurity subspace, i.e. $N_{\text{ref}} = (N_c C_{N_c/2})^2$ where ${}_n C_m = n!/(m!(n-m)!)$, so that while the computational complexity grows exponentially in the size of the impurity Hilbert space, it scales only as a power of the number of bath orbitals and the reduced dimension of the Hilbert space in CI means the prefactor is smaller. Studies of up to $N_b = 20$ are possible for a four-site cluster without parallelization for distributed memory system; larger systems should be accessible when the algorithm is optimized.

Figure 1 shows the density of states (DOS) ρ obtained from converged DMFT solutions for different number of bath states N_b . As is standard in ED calculations, a small broadening factor $\eta = 0.10\text{eV}$ is introduced and ρ is defined in terms the trace of the branch cut discontinuity of the local Green function:

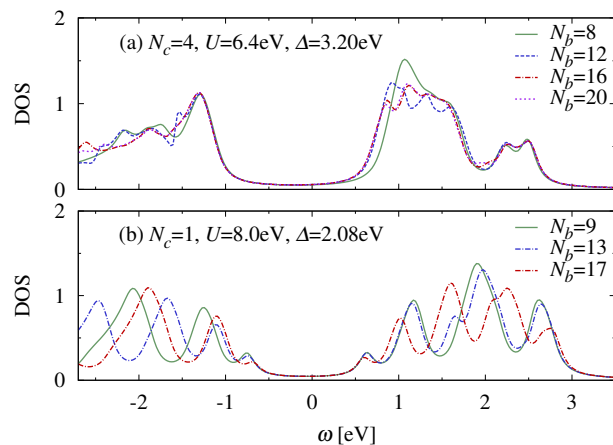


FIG. 1. (color online) Density of states from (a) 4-site and (b) single-site DMFT with various values of N_b . A small broadening factor $\eta = 0.10\text{eV}$ is used.

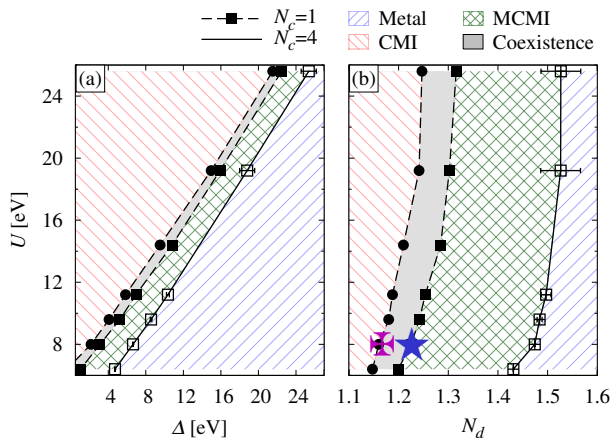


FIG. 2. (color online) Metal-insulator transition phase diagram in plane of interaction strength U and p - d energy splitting Δ (panel (a)) and d -occupancy N_d (panel (b)) from single-site ($N_c = 1$) and 4-site ($N_c = 4$) dynamical mean field approximation. The error bars reflect uncertainties arising from restricting to $P = 2$ particle-hole pairs at large U ; where not shown they are smaller than the size of the points. The region shaded with lines slanting up and to the left is the conventional Mott insulator (CMI) region, where insulating behavior is found even for $N_c = 1$; the region shaded with lines slanting up and to the right indicate regions that are metallic in the single-site approximation and the cross-hatched region is the magnetically correlated Mott insulator (MCMI), which is insulating for $N_c = 4$ but not $N_c = 1$. The shaded area is the coexistence region of the metal-insulator transition in the single-site approximation. The symbols ‘✕’ and ‘★’ denote parameter values that yield gaps comparable to the experimental values for $N_c = 1$ and 4 respectively.

$\rho(\omega) = \text{Tr} [\mathbf{G}_{\text{loc}}(\omega - i\eta) - \mathbf{G}_{\text{loc}}(\omega + i\eta)] / (2\pi i)$. \mathbf{G}_{loc} is the 12×12 matrix (4 momentum space tiles and three orbitals per tile) defined in Eq. 5 of the supplementary material. Consistent with previous work [35], our single-site calculations (lower panel) show that $N_b = 9$ is sufficient to describe the behavior at gap edge. For the four-site case we verify that $N_b = 8$ produces qualitatively correct results, but leads to errors in the spectral gap of $\sim 0.2\text{eV}$, while for $N_b = 12$ the spectral gap is quantitatively converged. In the rest of the paper we use $(N_c, N_b) = (1, 9)$ and $(4, 12)$ unless otherwise mentioned.

In the left panel of Fig. 2 we present the metal insulator phase diagram obtained by single-site and cluster DMFT method in the plane of interaction strength and charge transfer energy at total filling $n = 5$ (one hole per Cu). To determine the nature (metallic vs insulating) of the state we examine the low frequency behavior of the self energy. For an insulator, the self energy has a pole near the chemical potential, while for a metal the self energy is smooth. This criterion is less sensitive to finite-bath size errors than is a direct examination of the density of states. The single-site approximation contains the physics of conventional Mott/charge transfer insulators,

while the cluster approximation additionally includes the effects of intersite correlations. Comparison of the two allows us to distinguish different types of insulators.

The single-site results are consistent with previous work [35]. The transition is first order; the coexistence region is shaded in Fig. 2. The size of this coexistence region is robust against increasing N_b . The four-site approximation widens the insulating regime, shifting the phase boundary in the $U - \Delta$ plane to the right by about $\delta\Delta = 3\text{eV}$. The shift indicates that (as also found in the Hubbard model [10, 19, 36, 37]) intersite magnetic correlations present in the $N_c = 4$ but not the $N_c = 1$ calculation play a crucial role in stabilizing the insulating state. We designate the region which is insulating only if intersite correlations are included as the magnetically correlated Mott insulator (MCMI) and the region which is insulating even in the single-site approximation as the conventional Mott insulator (CMI). As in the 4-site approximation to the Hubbard model [36, 37], the transition in the four-site approximation to the p - d model is found to be weakly first order, with a small coexistence region; however the size of the coexistence region shrinks as the number of bath states is increased (not shown) and the actual size of the coexistence region for this model is not established by the results we have.

Previous work [38] has shown that it is useful to consider the physics as a function of the d -occupancy N_d . In p - d models of the kind studied here, results expressed in terms of N_d are insensitive to such details of the band structure as the oxygen-oxygen hopping. The right panel of Fig. 2 shows the metal-insulator phase diagram in the plane of interaction strength and d -occupancy. Inclusion of intersite correlations shifts the phase boundary by about 0.25 in N_d , with the shift being independent of U . The ability of the CI method to attain larger U allows us to see that the phase boundary in the $U - N_d$ plane only becomes vertical for very large $U \sim 16\text{eV}$, while physically relevant values for the copper-oxide materials are ~ 8 – 10eV [1].

In Fig. 3 we present the excitation gap determined from the calculated self energy and the quasiparticle equation as discussed in Ref. [39]. In the single-site approximation, at fixed U the gap magnitude in the insulating solution decreases linearly as N_d increases. This smooth behavior indicates that there is only one kind of insulating state in the single-site approximation. We identify this as the conventional Mott insulator (CMI) phase. As extensively discussed [11], the gap in the CMI phase can be smoothly decreased to zero but this transition is preempted by a first order transition to a metallic phase. In the four-site approximation, two regimes are evident: a small N_d strongly correlated regime where the gap vs N_d curve is very similar to the single-site approximation (albeit with an enhanced gap) and a larger N_d regime where the slope of the $\Delta - N_d$ curve changes. We identify this regime as the MCMI. The crossover between the two regimes

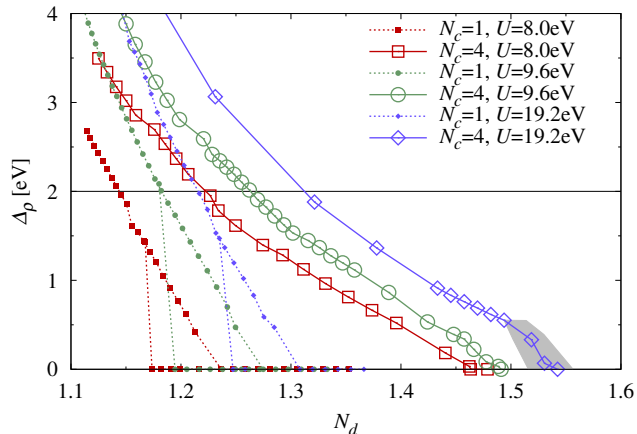


FIG. 3. (color online) Spectral gap as a function of d -occupancy for various values of U with $(N_c, N_b) = (1, 9)$ and $(4, 12)$. For $N_c = 1$, two distinct solutions depending on initial conditions are shown in the intermediate region. The black horizontal line indicates the charge transfer gap $\Delta_\rho = 2\text{eV}$ characteristic of the parent compounds of the high- T_c cuprates. The size of the shaded region reflects the uncertainties arising from the $P = 2$ approximation at large U .

occurs at the point at which the gap closes in the single-site approximation.

The optically determined [40] charge transfer gap of about 2eV is shown as a horizontal line. For U -values in the generally accepted range $U \sim 8\text{--}10\text{eV}$ we see that an $N_d \sim 1.14\text{--}1.20$ is required to reproduce the gap in the single-site approximation; in the 4-site approximation a larger $N_d \sim 1.22\text{--}1.28$ is needed to reproduce the gap. The N_d values needed to reproduce the insulating gap for $U = 8\text{eV}$ are marked in Fig. 2 by the symbols ‘✠’ (for the single-site case) and ‘★’ (in the four-site case). The N_d needed to fit the observed excitation gap in the 4-site approximation is in the coexistence region of the single-site approximation. Both in the 1-site and 4-site cases the N_d values required to account for the observed gap are substantially smaller than the density functional prediction $N_d \sim 1.4$ [38], suggesting that density functional theory overestimates the Cu-O covalence. An analysis of nuclear magnetic resonance data [41] suggests an $N_d \sim 1.22$ consistent with the $N_c = 4$ calculation.

Figure 4 presents the optical conductivity (a, b) and DOS (c) obtained for $U = 8\text{eV}$ with Δ values chosen to reproduce the observed $\sim 2\text{eV}$ gap. In the 4-site optical conductivity calculation, vertex corrections are incorporated following the method presented in Ref. [42]. We see that the single-site calculation predicts a very small value for the optical conductivity at frequencies not too far above the upper gap edge, while the four-site calculation yields a much larger conductivity for frequencies near the gap edge, in a better agreement with data [40]. The physics is that the gap is indirect and vertex corrections (not present in the $N_c = 1$ calculation) activate

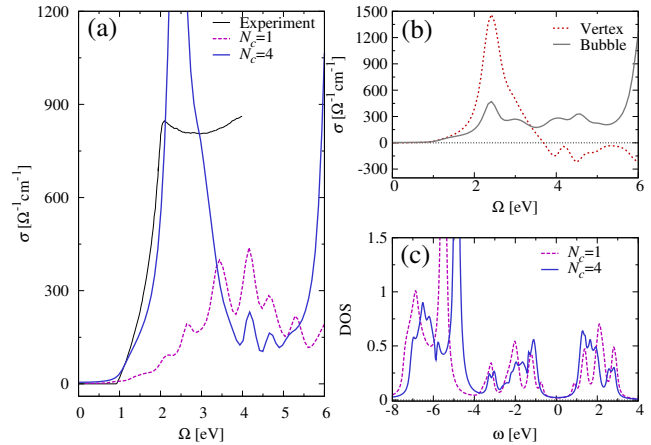


FIG. 4. (color online) (a) Optical conductivity from the single- and 4-site DMFT with parameters fixed to yield gap size $\Delta_\rho \sim 2\text{eV}$ at correlation strength $U = 8.0\text{eV}$ while the 4-site calculation leads to a rapid rise in the conductivity at the gap edge, in agreement with experiment. (b) Vertex and bubble contribution to the optical conductivity for 4-site DMFT. (c) Density of states with the same parameters in (a).

gap edge transitions by allowing for a multi-particle transition in which an excitation of momentum $\mathbf{Q} \approx (\pi, \pi)$ is emitted. The vertex corrections are present for all values of the correlation strength but are most important in the MCMI regime (see supplementary material). The large enhancement of the gap edge conductivity relative to experiment is an artifact of the $N_c = 4$ approximation, which concentrates the vertex corrections at the boundaries between momentum space tiles. The integrated spectral weight, which is more robust to details of methodology is in good agreement with data (see supplementary material).

In summary, this paper introduces an implementation of the Zgid-Chan CI-solver [12] which allows us to obtain converged real-frequency results for single-particle and conductivity spectra of the charge-transfer model generally agreed to represent the physics of the high- T_c cuprate superconductors, for a wide range of previously inaccessible parameters. Our results enable us to distinguish two types of insulating phase, the conventional Mott insulator and the magnetically correlated Mott insulator and comparison of our calculations to experiment place the materials in the magnetically correlated Mott insulator (MCMI) region of the phase diagram, supporting previous suggestions [8, 9, 38] that intersite correlations play an essential role in the physics of the high- T_c cuprates. A subsequent paper will investigate the different doping dependences of the two phases. Our work also resolves a previously noted [9] discrepancy between theory and optical conductivity data. Finally, we confirm previous indications [38] that single-site dynamical mean field theory provides a quantitatively poor approximation to

basic properties of the two dimensional charge-transfer model and that density functional band theory overestimates the p - d hybridization and should not be used as a guide for placing materials on the metal-charge transfer insulator phase boundary. Our work validates the CI method as a robust and powerful approach for investigating the physics of correlated electron materials. As a direction for future work we note that the ability of the CI method to treat a much larger number of bath orbitals than is possible in conventional ED solvers indicates that the method will be useful in treating the non-diagonal hybridization functions arising in low symmetry situations, where severe sign problems limit the applicability of quantum Monte Carlo methods [22] and difficulties with bath-fitting prevent the application of conventional ED methods. Spin-orbit coupled situations and cluster DMFT descriptions of systems with several partially occupied correlated orbitals may now be theoretically accessible.

This work was supported by the US Department of Energy under Grants No. DOE FG02-04ER46169 and DE-SC0006613.

-
- [1] M. Imada, A. Fujimori, and Y. Tokura, *Rev. Mod. Phys.* **70**, 1039 (1998).
- [2] P. W. Anderson, *Science* **235**, 1196 (1987).
- [3] F. C. Zhang and T. M. Rice, *Phys. Rev. B* **37**, 3759 (1988).
- [4] P. A. Lee, N. Nagaosa, and X.-G. Wen, *Rev. Mod. Phys.* **78**, 17 (2006).
- [5] C. Weber, K. Haule, and G. Kotliar, *Phys. Rev. B* **82**, 125107 (2010).
- [6] J. R. Schrieffer, X.-G. Wen, and S.-C. Zhang, *Phys. Rev. Lett.* **60**, 944 (1988).
- [7] A. Abanov, A. V. Chubukov, and J. Schmalian, *Europhys. Lett.* **55**, 369/375 (2001).
- [8] A. Comanac, L. de' Medici, M. Capone, and A. Millis, *Nature Physics* **4**, 287 (2008).
- [9] X. Wang, L. de' Medici, and A. J. Millis, *Phys. Rev. B* **83**, 094501 (2011).
- [10] T. Maier, M. Jarrell, T. Pruschke, and M. H. Hettler, *Rev. Mod. Phys.* **77**, 1027 (2005).
- [11] A. Georges, G. Kotliar, W. Krauth, and M. J. Rozenberg, *Rev. Mod. Phys.* **68**, 13 (1996).
- [12] D. Zgid and G. K.-L. Chan, *J. Chem. Phys.* **134**, 094115 (2011).
- [13] D. Zgid, E. Gull, and G. K.-L. Chan, *Phys. Rev. B* **86**, 165128 (2012).
- [14] J. Zaanen, G. A. Sawatzky, and J. W. Allen, *Phys. Rev. Lett.* **55**, 418 (1985).
- [15] V. J. Emery, *Phys. Rev. Lett.* **58**, 2794 (1987).
- [16] C. M. Varma, *Phys. Rev. B* **55**, 14554 (1997).
- [17] M. Karolak, G. Ulm, T. Wehling, V. Mazurenko, A. Poteryaev, and A. Lichtenstein, *J. Electron. Spectrosc. Relat. Phenom.* **181**, 11 (2010).
- [18] A. Macridin, M. Jarrell, T. Maier, and G. A. Sawatzky, *Phys. Rev. B* **71**, 134527 (2005).
- [19] E. Gull, M. Ferrero, O. Parcollet, A. Georges, and A. J. Millis, *Phys. Rev. B* **82**, 155101 (2010).
- [20] A. N. Rubtsov, V. V. Savkin, and A. I. Lichtenstein, *Phys. Rev. B* **72**, 035122 (2005).
- [21] P. Werner, A. Comanac, L. de' Medici, M. Troyer, and A. J. Millis, *Phys. Rev. Lett.* **97**, 076405 (2006).
- [22] E. Gull, A. J. Millis, A. I. Lichtenstein, A. N. Rubtsov, M. Troyer, and P. Werner, *Rev. Mod. Phys.* **83**, 349 (2011).
- [23] S. Fuchs, E. Gull, L. Pollet, E. Burovski, E. Kozik, T. Pruschke, and M. Troyer, *Phys. Rev. Lett.* **106**, 030401 (2011).
- [24] K. Haule, *Phys. Rev. B* **75**, 155113 (2007).
- [25] R. Bulla, T. A. Costi, and T. Pruschke, *Rev. Mod. Phys.* **80**, 395 (2008).
- [26] K. A. Hallberg, *Adv. Phys.* **55**, 477 (2006).
- [27] M. Caffarel and W. Krauth, *Phys. Rev. Lett.* **72**, 1545 (1994).
- [28] M. Capone, L. de' Medici, and A. Georges, *Phys. Rev. B* **76**, 245116 (2007).
- [29] A. Liebsch, H. Ishida, and J. Merino, *Phys. Rev. B* **78**, 165123 (2008).
- [30] A. Liebsch and N.-H. Tong, *Phys. Rev. B* **80**, 165126 (2009).
- [31] A. Liebsch and H. Ishida, *J. of Phys.: Condensed Matter* **24**, 053201 (2012).
- [32] M. Civelli, M. Capone, A. Georges, K. Haule, O. Parcollet, T. D. Stanescu, and G. Kotliar, *Phys. Rev. Lett.* **100**, 046402 (2008).
- [33] C. Lin and A. A. Demkov, *Phys. Rev. B* **88**, 035123 (2013).
- [34] A. Go and A. J. Millis, Unpublished.
- [35] L. de' Medici, X. Wang, M. Capone, and A. J. Millis, *Phys. Rev. B* **80**, 054501 (2009).
- [36] H. Park, K. Haule, and G. Kotliar, *Phys. Rev. Lett.* **101**, 186403 (2008).
- [37] E. Gull, P. Werner, X. Wang, M. Troyer, and A. J. Millis, *Europhys. Lett.* **84**, 37009 (2008).
- [38] X. Wang, M. J. Han, L. de' Medici, H. Park, C. A. Marianetti, and A. J. Millis, *Phys. Rev. B* **86**, 195136 (2012).
- [39] X. Wang, E. Gull, L. de' Medici, M. Capone, and A. J. Millis, *Phys. Rev. B* **80**, 045101 (2009).
- [40] S. Uchida, T. Ido, H. Takagi, T. Arima, Y. Tokura, and S. Tajima, *Phys. Rev. B* **43**, 7942 (1991).
- [41] J. Haase, O. P. Sushkov, P. Horsch, and G. V. M. Williams, *Phys. Rev. B* **69**, 094504 (2004).
- [42] N. Lin, E. Gull, and A. J. Millis, *Phys. Rev. B* **80**, 161105 (2009).